

## CONSTRAINED MULTISINE INPUTS FOR PLANT-FRIENDLY IDENTIFICATION OF CHEMICAL PROCESSES

D.E. Rivera,<sup>\*,1</sup> M.W. Braun<sup>\*</sup> and H.D. Mittelmann<sup>\*\*</sup>

*\* Control Systems Engineering Laboratory  
Department of Chemical and Materials Engineering  
\*\* Department of Mathematics  
Arizona State University, Tempe, Arizona 85287*

**Abstract:** This paper considers the use of *constrained* minimum crest factor multisine signals as inputs for plant-friendly identification testing of chemical process systems. The approach developed in this paper greatly increases their effectiveness in a process control setting by enabling the user to simultaneously specify important frequency and time-domain characteristics of these signals. Two problem formulations meaningful to both linear and nonlinear identification problems are presented. State-of-the-art computational methods are needed to solve the challenging optimization problems associated with crest factor minimization.

**Keywords:** “plant-friendly” system identification, chemical process control

### 1. INTRODUCTION

The concept of “plant-friendliness” in system identification stems from the fundamental need for informative experiments despite practical requirements to the contrary. A plant-friendly identification test will produce data leading to a suitable model within an acceptable time period, while keeping the variation in both input and output signals within user-defined constraints.

These practical considerations are often in conflict with theoretical requirements (e.g., identifiability, persistence of excitation, etc.) which demand long identification tests under high signal-to-noise ratios. As a result, plant-friendliness often involves a compromise between the demands of theory

(which are in large part “plant-hostile”) and the plant engineer’s desire for no changes in the process stemming from identification testing.

The main objective of this paper is to present a novel, systematic framework for plant-friendly identification centered on the use of *constrained* multisine inputs. Multisine signals are deterministic, periodic signals, represented in the single input case by the equation

$$u(k) = \lambda \sum_{i=1}^{n_s} \sqrt{2\alpha_i} \cos(\omega_i kT + \phi_i), \quad (1)$$
$$\omega_i = 2\pi i / N_s T, \quad n_s \leq N_s / 2$$

The power spectrum in a multisine input can be directly specified by the user through the selection of the scaling factor  $\lambda$ , the Fourier coefficients  $\alpha_i$ , the number of harmonics  $n_s$ , and the signal length

---

<sup>1</sup> to whom all correspondence should be addressed;  
phone:(480) 965-9476, email:daniel.rivera@asu.edu

$N_s$ .  $T$  is the sampling time. Multisine inputs are easy to implement in a real-time setting; as deterministic signals, one cycle can be designed to include all the frequency content needed for consistent estimation of the plant dynamics. Under noisy testing conditions, multiple cycles can be implemented until the variance in the model estimate is reduced to acceptable levels (Ljung, 1999).

The Crest Factor ( $CF$ ) of a signal  $u$  is the ratio of the  $\ell_\infty$  (or Chebyshev) norm and the  $\ell_2$ -norm

$$CF(u) = \frac{\ell_\infty(u)}{\ell_2(u)} \quad (2)$$

It provides a measure of how well distributed the signal values are over the input span. A low crest factor indicates that most of the elements in the input sequence are distributed near the minimum and maximum values of the sequence. Reducing the crest factor of an input signal can significantly improve the signal to noise ratio of the resulting plant output, contributing to plant-friendliness during experimental testing.

In this paper, we present a novel design procedure for multisine input signals which addresses the requirements of process control practice and can thus enable informative, plant-friendly identification in the process industries. The methodology presented here effectively integrates operating restrictions, identification-theoretic requirements, and sophisticated optimization techniques to design minimum crest factor multisine signals satisfying important user-specified time and frequency domain properties.

The optimization problem of minimizing the crest factor of a signal under time domain constraints represents a challenging computational task, but is critical to the success of the proposed technique. For one, it is always nonlinear, either in the objective function, the constraints or in both. It is nonconvex in general from the statement of the objective function. In addition it is nonsmooth as a consequence of the  $\ell_\infty$  norm in the objective function. Combined with its size in terms of both variables and constraints, this problem requires the use of state-of-the art optimization techniques. Ultimately, our goal is to develop a solution technique that is amenable to real-time computation and is thus consistent with the needs of the practicing engineer.

## 2. BACKGROUND AND PROPOSED FRAMEWORK

Early work in the design of low crest factor multisines for system identification comes from the work of Schroeder (1970), who derives a closed-form formula to select the phases in (1)

$$\phi_i = 2\pi \sum_{j=1}^i j\alpha_j \quad (3)$$

The formula gives a reasonable result when the user-defined spectrum is flat and wideband, but under other conditions (bandlimited, in the presence of harmonic suppression, etc.) the results can be very undesirable.

The deficiencies of Schroeder-phasing justify the need for more rigorous approaches, such as those involving optimization. A significant contribution in this regard is the work by Guillaume *et al.* (1991). This method seeks to approximate the minimization of the Chebyshev norm by sequentially minimizing the  $\ell_p$  norm for  $p = 4, 8, 16, \dots$ . It is based on Pólya's algorithm which states that

$$\lim_{p \rightarrow \infty} \mathbf{p}_p = \mathbf{p}_\infty \quad (4)$$

where  $\mathbf{p} = [\phi_2 \ \phi_3 \ \dots \ \phi_{n_s}]$  is the real-valued phase vector for (1) and  $\mathbf{p}_\infty$  is the minimax solution. Note that the  $\ell_2$ -norm remains invariant with respect to the phases  $\phi_i$ . A discrete-time representation of the  $\ell_p$  norm is incorporated into a Gauss-Newton optimization algorithm with Levenberg-Marquardt Hessian approximation. This is accomplished by defining a cost function

$$\min_{\mathbf{p}} \frac{1}{N_s} e^T e, \quad (5)$$

where  $(6)$

$$\begin{aligned} e &= [u_s(1)^{p/2} \ u_s(2)^{p/2} \ \dots \ u_s(N_s)^{p/2}]^T \\ \mathbf{p} &= [\phi_2 \ \phi_3 \ \dots \ \phi_{n_s}]^T \end{aligned}$$

and  $p$  is an even number. The elements of the Jacobian  $\mathbf{J}$  can be represented by

$$J_{ki} = -(p/2)u_s(k)^{(p/2-1)}\sqrt{(2\alpha_i)}\sin(\omega_i kT + \phi_i),$$

which form part of the iterative phase update equation

$$\begin{aligned} \mathbf{p}^{(i)} &= \mathbf{p}^{(i-1)} - [\mathbf{J}^{(i-1)T} \\ &\quad \mathbf{J}^{(i-1)} + \Lambda^{(i-1)}]^{-1} \mathbf{J}^{(i-1)T} e^{(i-1)} \end{aligned} \quad (7)$$

An FFT-based algorithm is used to compute  $\mathbf{J}^{(i-1)T} \mathbf{J}^{(i-1)}$  and  $\mathbf{J}^{(i-1)T} e^{i-1}$ . The sequential optimization process in Guillaume *et al.* is initialized with the phases produced by the Schroeder-phase algorithm. Although a global solution cannot be guaranteed with this approach, most local minima are avoided and Guillaume *et al.* report that it performs better than other crest factor minimization techniques.

While the Guillaume *et al.* algorithm is useful, its applicability to process control problems has some important limitations. The user must accept whatever time-domain realization is produced by

the algorithm, and is not able to specify time-domain constraints which may be demanded by plant-friendliness considerations. Hererin lies the main motivation for the constrained problem formulations developed in this paper.

A solution approach to the constrained minimum crest factor multisine problem can take a variety of forms. An initial approach that we propose is similar to the one used by Guillaume and co-workers and is based on Pólya’s algorithm. First, the problem is formulated in the modeling language AMPL. This has obvious advantages over a formulation in any high-level programming language including the possibility to utilize for its solution a number of available solvers which themselves are written in various languages. However, a more important benefit results from the fact that AMPL has built-in automatic derivatives and that means exact and efficient differentiation up to second derivatives.

Next, we minimize a properly scaled (to avoid underflow or overflow)  $p$ -norm instead of the Chebyshev norm. Different from Guillaume *et al.* (1991), we use an elaborate technique to increase  $p$ . Essentially, through a more gradual increase of  $p$ , a long sequence of optimization problems is generated. While in principle an active-set method of sequential quadratic programming type (generally still considered state-of-the art for general nonlinear programming) could be used, we have turned to interior point methods. The reason is that these methods are more effective for large problem sizes, particularly those that would arise in multivariable cases.

A series of novel interior point approaches have been recently proposed and partly been made available by their authors. A very successful class of methods is that of primal-dual methods. This is certainly true for linear and quadratic programming. For general nonlinear programming it has been shown in (Wächter and L.T. Biegler, 2000) that typical, line search based interior point methods may fail to converge to feasible points even for well-posed problems. One of the few methods that does not suffer from this is the trust region based method developed by Nocedal and co-workers which very recently was made available for research purposes (Byrd *et al.*, 1999). This method possesses the robustness and stability needed for our purposes and at the same time is very efficient for smaller and larger problems. It has been used to generate all the results presented in this paper.

In the ensuing subsections, we present two practical problem formulations that can be meaningfully addressed via a constrained optimization solution. Numerical examples are presented to justify the usefulness of such an approach.

## 2.1 Problem 1: Minimizing crest factor with respect to multisine phases only, subject to move size and output variability constraints

Given a multisine signal of the form in Equation (1) and a power spectrum (defined by the Fourier coefficients  $\lambda\sqrt{2\alpha_i}$  for  $n_s$  spectral lines), this problem calls for searching for the phases that minimize the crest factor

$$\min_{[\phi_2 \ \phi_3 \ \dots \ \phi_{n_s}]} \text{CF}(u) \quad (8)$$

subject to maximum move size constraints on the input,

$$|\Delta u(k)| \leq \Delta u^{max} \quad \forall k \quad (9)$$

and possibly high/low limits on  $u(k)$ ,

$$u^{min} \leq u(k) \leq u^{max} \quad \forall k \quad (10)$$

As an example we consider a first-order with deadtime plant model (with input  $u$  and output  $y$ ) with parameters

$$\frac{y(s)}{u(s)} = p(s) = \frac{Ke^{-\theta s}}{\tau s + 1} = \frac{e^{-3s}}{3s + 1} \quad (11)$$

The system is sampled at the rate of  $T = 1$  minute. Figure 1 shows a control-relevant power spectrum obtained from the work of Rivera *et al.* (1992) for the plant described by (11) using a dominant time constant estimate  $\tau_{dom} = 4.5$  min and a desired closed-loop speed of response  $\tau_{cl} = 2.25$  min. Figure 2 and Tables 1 and 2 summarize the results of the Schroeder-phased design. The multisine signal with phases chosen per Equation (3) produces a time-domain realization with rather high crest factor (2.7966) and a large maximum move size (1.6214). Examining Figure 2 one notes that the signal is unevenly distributed and exhibits rather wide overall input and output spans.

Figure 2 and Tables 1 and 2 show the result of the Guillaume *et al.* algorithm for the design of a multisine input with control-relevant power spectrum according to Figure 1. This “Guillaume-phased” input has significantly lower input crest factor ( $\text{CF}(u) = 1.2173$ ) and maximum move size ( $\max(\Delta u) = 1.1013$ ) than its Schroeder-phased counterpart. This signal has “plant-friendly” properties in that the peaks of the signal are significantly compressed, resulting in a signal which is evenly distributed over the input range. The benefits are observed in reduced spans for both the input and output signals.

We apply the proposed approach for the case in which the maximum input move size is constrained to  $\Delta u^{max} = 0.52$ . This constraint represents a significant reduction (less than half)

the maximum move size experienced from the Guillaume-phased signal. The approach is applied and the signals are compared in Figure 2 and Tables 1 and 2. While the constrained signal experiences an unavoidable increase in crest factor (from 1.2173 to 1.5388), the overall input span does not change dramatically and the net increase on the output span is relatively small. Even under constrained conditions, the signal displays substantially better characteristics than the Schroeder-phased input.

It is also possible to consider a scenario in which the crest factor for the output signal is minimized.

$$\min_{[\phi_2 \ \phi_3 \ \dots \ \phi_{n_s}]} \text{CF}(y) \quad (12)$$

This scenario assumes that some *a priori* knowledge of the model (in either parametric or non-parametric form) is available to the optimizer to generate predicted outputs. One possible source for such a model is the result of parameter estimation applied to data collected from previous cycles of the multisine input. In addition to the constraints listed in Equations (9) and (10), the problem is also subject to output variability constraints

$$|\Delta y(k)| \leq \Delta y^{max} \quad \forall k \quad (13)$$

and high/low limits on  $y(k)$

$$y^{min} \leq y(k) \leq y^{max} \quad \forall k \quad (14)$$

The results for the first-order with deadtime model parameters are shown in Tables 1 and 2 and Figure 3. First, we consider the results of minimizing the output crest factor in the absence of constraints. By minimizing the output crest factor, the overall span in the output is kept lower than that of any of the other input signal designs considered (Table 2). While this is highly desirable from the standpoint of reducing variation in the output signal, this is accomplished at the expense of large move sizes (and crest factor) in the input signal  $u$ . The constrained formulation, however, offers the user the opportunity to enforce limits on both input and output signals stemming from plant-friendly considerations. Both input move size and output variability constraints can be enforced; in our example, we set  $\Delta u^{max} = 0.6$  and  $\Delta y^{max} = 0.45$ . Results are shown in Figure 3 and Tables 1 and 2. The constrained solution achieves the desired tradeoffs: the maximum move size in the input signal is lowered substantially as a result of constraints, while the output variability and span are kept within acceptable levels. This flexibility is of significant benefit to the user.

## 2.2 Problem 2: Minimizing crest factor with respect to phases and Fourier coefficients subject to move size and output variability constraints

A more general multisine input structure that benefits from a constrained problem formulation is the signal according to the equation:

$$u(k) = \lambda \sum_{i=1}^{n_s} \sqrt{2\alpha_i} \cos(\omega_i kT + \phi_i) \quad (15) \\ + \sum_{i=n_s+1}^{n_a+n_s} \hat{a}_i \cos(\omega_i kT + \phi_i^a)$$

where  $n_a + n_s \leq N_s/2$  and  $\hat{a}_i$  and  $\phi_i^a$  represent the Fourier coefficients and phases, respectively, for  $n_a$  spectral lines beyond those defined in the user-specified spectrum. As noted in Guillaume *et al.* (1991), the presence of these additional sinusoids creates a “snow effect” that will increase the energy content of the signal and contribute to a decrease in the crest factor. For the structure per (15), the constrained optimization problem consists of searching for  $\phi_i$ ,  $\hat{a}_i$ , and  $\phi_i^a$  to minimize the crest factor (of either  $u$  or  $y$ ) subject to constraints as noted in Equations (9), (10), (13), and (14).

Figure 4 presents a general diagram for an input signal design relevant to the structure represented in Equation (15). In Figure 4 a “flat” low-pass frequency spectrum is defined over the control-relevant frequency range, which can be defined by guidelines relying on *a priori* information, as presented in (Braun *et al.*, 2000). In this guideline, the control-relevant frequency range is defined by

$$\omega_* = \frac{1}{\beta_s \tau_{dom}^H} \leq \omega \leq \frac{\alpha_s}{\tau_{dom}^L} = \omega^* \quad (16)$$

$\tau_{dom}^H$  and  $\tau_{dom}^L$  correspond to the high and low estimates of the dominant time constant of the system.  $\alpha_s$  and  $\beta_s$  correspond to user-decisions on the high and low frequency content of the signal, respectively. Per Figure 4, the user can choose to suppress multiples of 2, 3, or 5 in the Fourier coefficients of  $\alpha_i$  to minimize the effect of nonlinear plant behavior in the identification of linear dynamics (Godfrey, 1993). The ability of the optimizer to adjust the phase and magnitude of the high frequency sinusoids while keeping the input and output signals within time-domain constraints is expected to significantly reduce the crest factor while maintaining plant-friendly operation.

The problem formulation is exemplified using the multisine input design developed for the CSTR case study presented in (Braun *et al.*, 2000). The power spectrum considered in (Braun *et al.*, 2000)

for the case of even harmonic suppression (with high frequency harmonics preset to a fraction of the lower frequency values) corresponds to Case 1 in Figure 5. As noted in Table 3 and Figure 6, the input resulting from an unconstrained optimization per Equation (8) experiences a rather large maximum move size of 2.2618. Enforcing a constraint of  $\Delta u^{max} = 0.8$  while using the same power spectrum (i.e., without optimizing on the high frequency Fourier coefficients) unavoidably increases both the crest factor and the overall span; these are the Case 2 results in Figure 5 and 6 and Table 3. However, given the ability to optimize on both the phases and high frequency Fourier coefficients (Case 3), the crest factor and overall span are lowered dramatically; the resulting signal is superior to the two inputs presented in Cases 1 and 2.

### 3. SUMMARY

The paper describes an enhanced formulation of the minimum crest factor multisine problem that allows users to simultaneously specify important frequency and time domain properties of multisine signals. As a result, the input signals arising from this technique are meaningful for accomplishing plant-friendly identification in the process industries. Two problem formulations are shown and demonstrated via numerical examples.

### 4. REFERENCES

- Braun, M.W., R. Ortiz-Mojica, and D.E. Rivera (2000). *Proc. SYSID 2000*, pgs. 1097-1102; also *Control Engineering Practice*, in press.
- Byrd, R., M.E. Hribar, and J. Nocedal (1999). *SIAM J. Optim.* 9, pgs 877–900.
- Godfrey, K., Ed. (1993). *Perturbation Signals For System Identification*. Prentice Hall.
- Guillaume, P., J. Schoukens, R. Pintelon and I. Kollár (1991). *IEEE Trans. on Inst. and Meas.*, **40**(6), 982-989.
- Ljung, L. (1999) *System Identification: Theory for the User*, 2nd Edition, Prentice-Hall.
- Rivera, D.E., J.F. Pollard, and C.E. García, (1992) *IEEE Trans. Autom. Cntrl.*, **37**, 964-974.
- Schroeder, M. R. (1970). *IEEE Trans. Info. Theory*, vol. IT-16, pp. 85-89.
- Wächter, A. and L.T. Biegler (2000). *Math. Progr.* 88, pgs. 565–574.

Signal	CF( $u$ )	max( $\Delta u$ )	min( $u$ )	max( $u$ )
Schroeder-phased	2.7966	1.6214	-1.6384	1.75
Guillaume-phased	1.2173	1.1013	-0.7618	0.7612
min CF( $u$ ) Constrained ( $\Delta u^{max} = 0.52$ )	1.5388	0.5189	-0.9606	0.9628
min CF( $y$ ) Unconstrained	2.8144	1.5726	-1.5191	1.7611
min CF( $y$ ) ( $\Delta u^{max} = 0.6$ ; $\Delta y^{max} = 0.45$ )	2.1826	0.5156	-1.3571	1.3656

Table 1. Problem 1 example results summary for the input signal  $u$ .

Signal	CF( $y$ )	max( $\Delta y$ )	min( $y$ )	max( $y$ )
Schroeder-phased	2.5892	0.4846	-1.0524	0.9984
Guillaume-phased	1.7020	0.3506	-0.6918	0.6835
min CF( $u$ ) Constrained ( $\Delta u^{max} = 0.52$ )	1.7635	0.3348	-0.6693	0.7168
min CF( $y$ ) Unconstrained	1.2068	0.5745	-0.4851	0.4905
min CF( $y$ ) ( $\Delta u^{max} = 0.6$ ; $\Delta y^{max} = 0.45$ )	1.9633	0.3371	-0.7730	0.7980

Table 2. Problem 1 example results summary for the output signal  $y$ .

Signal	CF( $u$ )	max( $\Delta u$ )	min( $u$ )	max( $u$ )
Case 1	1.2274	2.2618	-1.8164	1.8164
Case 2	1.6854	0.8	-2.4942	2.4942
Case 3	1.0947	0.8	-1.6532	1.6532

Table 3. Problem 2 example results; Case 1 (unconstr.), Case 2 ( $\Delta u^{max} = 0.8$ ), Case 3 ( $\Delta u^{max} = 0.8$ ; Fourier coeff. optimized)

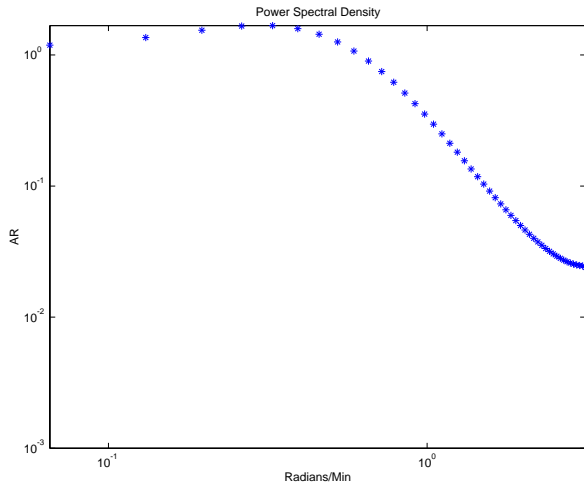


Fig. 1. Control-relevant spectrum, Problem 1 example;  $\tau_{dom} = 4.5$  min and  $\tau_{cl} = 2.25$  min.

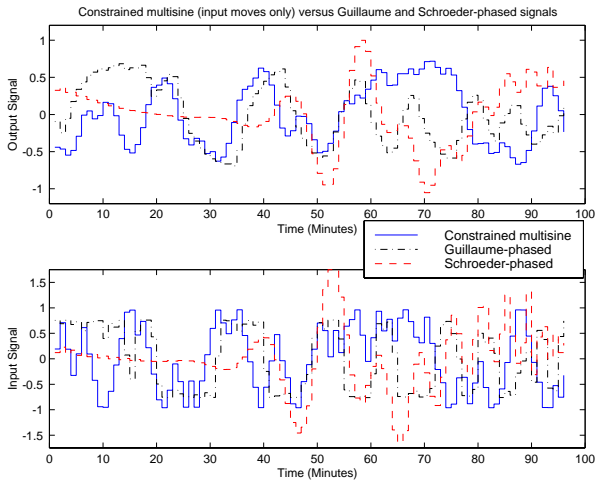


Fig. 2. Constrained multisine input signal (with  $\Delta u^{max} = 0.52$ ) compared to Guillaume-phased and Schroeder-phased signals, Problem 1 example.

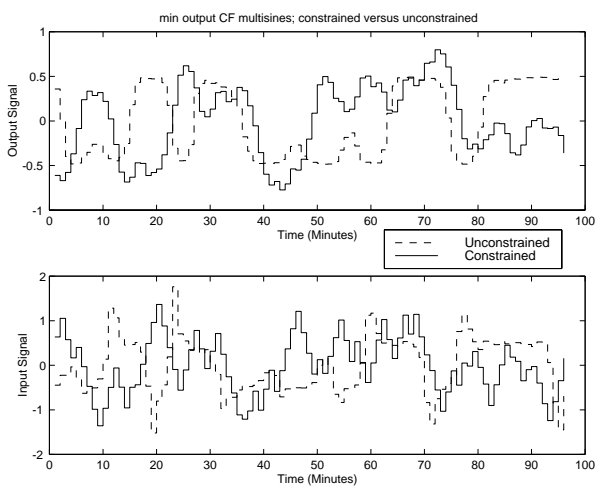


Fig. 3. Minimum *output* crest factor multisine inputs (constrained and unconstrained), Problem 1 example.

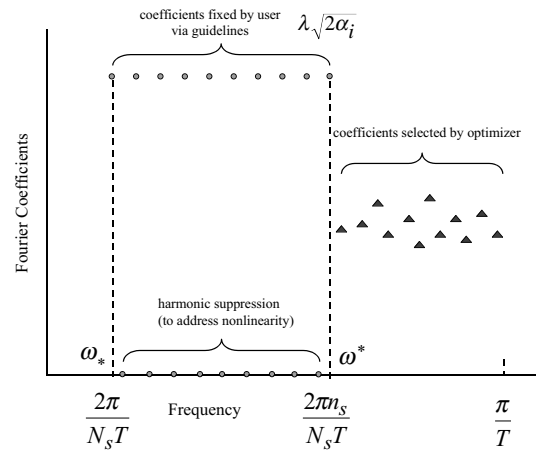


Fig. 4. Flat spectrum displaying harmonic suppression with optimized Fourier coefficients

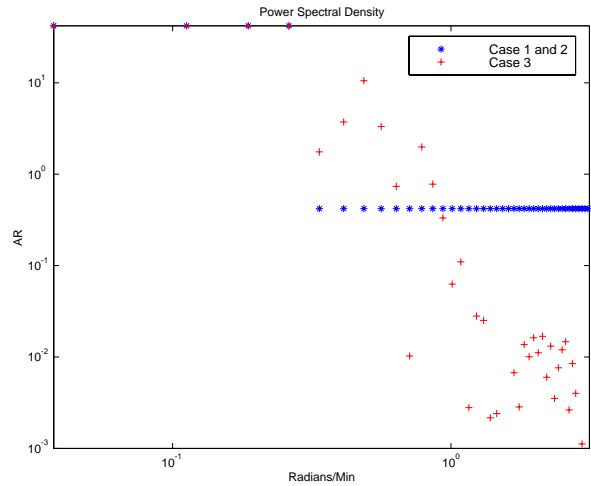


Fig. 5. Problem 2 example spectra; Case 1 (unconstr.), Case 2 ( $\Delta u^{max} = 0.8$ ), Case 3 ( $\Delta u^{max} = 0.8$ ; Fourier coeff. optimized)

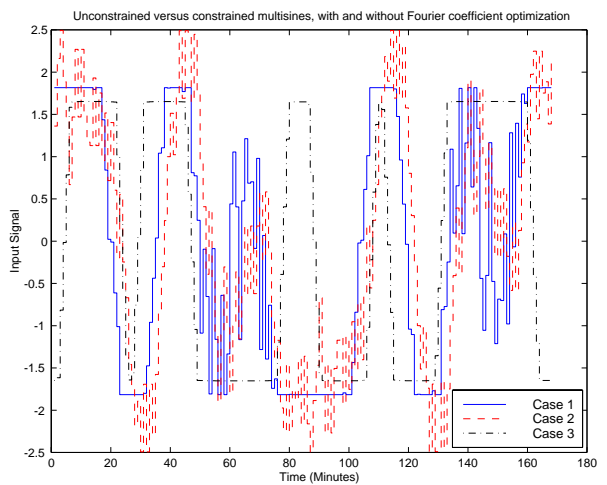


Fig. 6. Problem 2 example signals; Case 1 (unconstr.), Case 2 ( $\Delta u^{max} = 0.8$ ), Case 3 ( $\Delta u^{max} = 0.8$ ; Fourier coeff. optimized)